



# Time Resolution of the 4H-SiC PIN Detector

Tao Yang<sup>1,2</sup>, Yuhang Tan<sup>1,2</sup>, Qing Liu<sup>3</sup>, Suyu Xiao<sup>1,2,4</sup>, Kai Liu<sup>1</sup>, Jianyong Zhang<sup>1</sup>, Ryuta Kiuchi<sup>1</sup>, Mei Zhao<sup>1</sup>, Xiyuan Zhang<sup>1</sup>, Congcong Wang<sup>1</sup>, Boyue Wu<sup>5</sup>, Jianing Lin<sup>6</sup>, Weimin Song<sup>6</sup>, Hai Lu<sup>3\*</sup> and Xin Shi<sup>1\*</sup>

<sup>1</sup>Institute of High Energy Physics, Chinese Academy of Sciences, Beijing, China, <sup>2</sup>School of Physical Sciences, University of Chinese Academy of Sciences, Beijing, China, <sup>3</sup>School of Electric Science and Engineering, Nanjing University, Nanjing, China, <sup>4</sup>Shandong Institute of Advanced Technology, Jinan, China, <sup>5</sup>School of Physical Science and Technology, Guangxi University, Guangxi, China, <sup>6</sup>College of Physics, Jilin University, Jilin, China

We address the determination of the time resolution for the 100  $\mu\text{m}$  4H-SiC PIN detectors fabricated by Nanjing University (NJU). The time response to  $\beta$  particles from a  $^{90}\text{Sr}$  source is investigated for the detection of the minimum ionizing particles (MIPs). We study the influence of different reverse voltages, which correspond to different carrier velocities and device sizes, and how this correlates with the detector capacitance. We determine a time resolution  $(94 \pm 1) \text{ ps}$  for a 100  $\mu\text{m}$  4H-SiC PIN detector. A fast simulation software, termed RASER (RAdiation SEMiconductoR), is developed and validated by comparing the waveform obtained from simulated and measured data. The simulated time resolution is  $(73 \pm 1) \text{ ps}$  after considering the intrinsic leading contributions of the detector to time resolution.

**Keywords:** time resolution, 4H-SiC, MIP, simulation, Shockley–Ramo theorem

## INTRODUCTION

In the recent years, much attention has been devoted to seek the appropriate semiconductor material to be used in future particle colliders and nuclear reactors operating in harsh radiation environment (i.e.,  $> 10^{17} \text{ n}_{\text{eq}}/\text{cm}^2$ ) [1]. Silicon-based detectors have the support of a sophisticated production technology and present good quality, but the leakage current sharply increases and charge collection efficiency rapidly decreases when the irradiation fluence exceeds  $10^{15} \text{ n}_{\text{eq}}/\text{cm}^2$  [2]. To enhance performance and lifetime, most of the silicon-based detectors also need an expensive cooling system, which makes the overall detector system giant and expensive. Alternative diamond detectors have been investigated with high radiation hardness up to  $3 \times 10^{15} \text{ particles}/\text{cm}^2$  [3] and have been successfully used in the ATLAS experiment at the LHC [4]. However, they are also characterized by high cost and a difficult doping process in diamond, which limit their application. On the other hand, the 4H-SiC material, owing to its potential high radiation hardness, wide bandgap energy (3.27 eV), high atomic displacement energy (25 eV), and stability at high temperature, has great potential for application in extreme radiation environments.

Owing to the currently achieved high-quality 4H-SiC epitaxy wafer, a handful of studies about charge collection, leakage current, capacitance, and deep energy levels of 4H-SiC detectors have been carried out before and after irradiation [5, 6]. Due to its wide bandgap energy, which is also insensitive to visible light, SiC detectors are useful for X-ray and ultraviolet monitoring [7]. There have also been extensive studies about the SiC detector's application in neutron detection in fusion devices [6, 8]. Concerning applications in high-energy physics, the detector's response to the MIPs

## OPEN ACCESS

### Edited by:

Zheng Li,  
Ludong University, China

### Reviewed by:

Andrea Castoldi,  
Politecnico di Milano, Italy  
Anders Hallén,  
Royal Institute of Technology, Sweden

### \*Correspondence:

Hai Lu  
hailu@nju.edu.cn  
Xin Shi  
shixin@ihep.ac.cn

### Specialty section:

This article was submitted to  
Radiation Detectors and Imaging,  
a section of the journal  
Frontiers in Physics

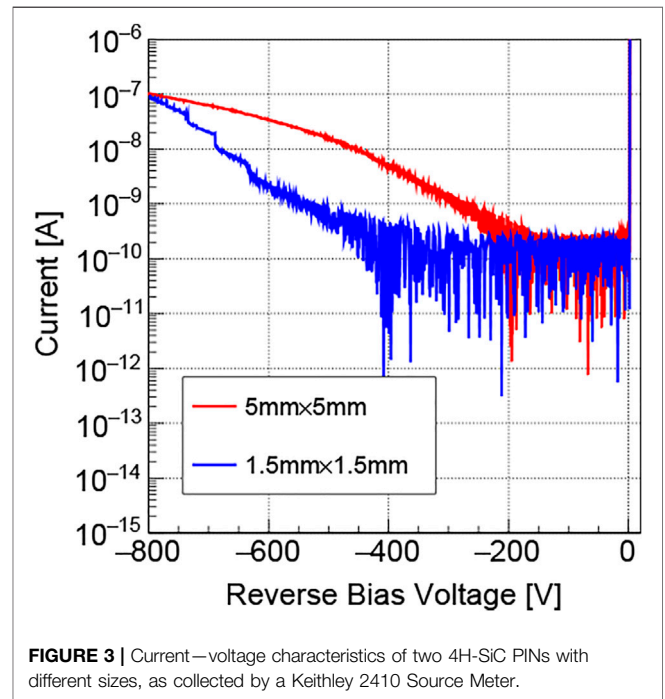
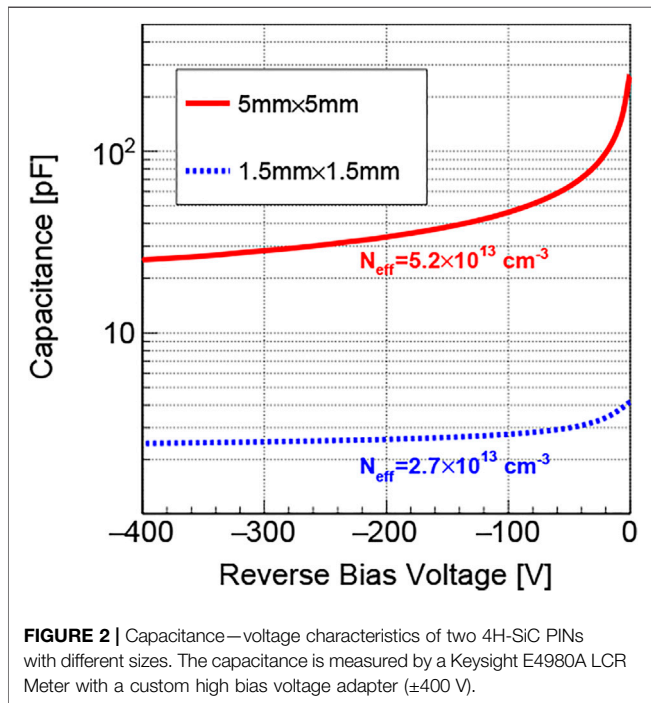
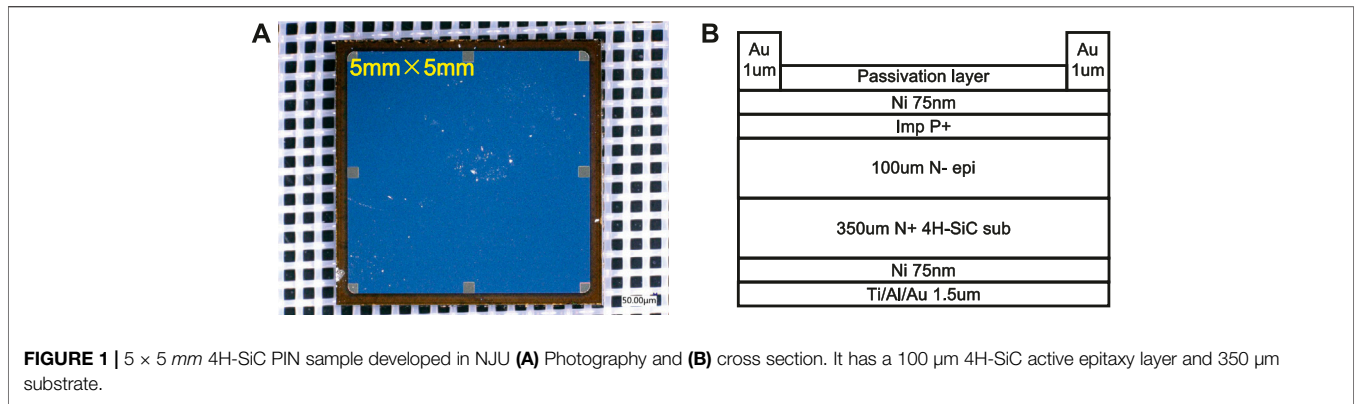
**Received:** 31 May 2021

**Accepted:** 25 January 2022

**Published:** 10 March 2022

### Citation:

Yang T, Tan Y, Liu Q, Xiao S, Liu K, Zhang J, Kiuchi R, Zhao M, Zhang X, Wang C, Wu B, Lin J, Song W, Lu H and Shi X (2022) Time Resolution of the 4H-SiC PIN Detector. *Front. Phys.* 10:718071. doi: 10.3389/fphy.2022.718071



is more relevant, but most of the previous studies focused on energy resolution and charge collection efficiency using  $\alpha$  particles, which are distinct features from the MIPs. To the best of our knowledge, charge collection features relevant to MIPs in SiC detectors have been analyzed [9], but no investigations about time resolution have been reported, except for the 4H-SiC Schottky barrier diode (SBD), where time resolution with  $\alpha$  particles for deuterium–tritium (D-T) applications has been analyzed [10].

In the recent years, ultrafast detectors have become a hot research topic. The main goal is to achieve a very high time and position resolution, simultaneously. A time resolution better than  $20 \text{ ps}$  has been achieved in silicon planar sensors with depletion thicknesses  $133\text{--}285 \mu\text{m}$  for multiple MIP signals [11], whereas  $100 \mu\text{m}$  silicon pixel detectors with  $800 \mu\text{m} \times 800 \mu\text{m}$  size have achieved a time resolution of  $106 \text{ ps}$  [12]. Currently,  $50 \mu\text{m}$  silicon detectors with internal gain, usually referred to as Low Gain

Avalanche Detector (LGAD), are developed by various foundries and show a time resolution of at least  $50 \text{ ps}$  [13–18]. The 4H-SiC detectors also show fast time response, coming from the highly saturated carrier velocity, but no time performance study has been reported so far.

Motivated by the abovementioned arguments, we here investigate the time resolution of the 4H-SiC PIN device using a  $^{90}\text{Sr}$  source for applications in high-energy physics experiments.

A fast simulation environment to investigate time resolution is a beneficial tool to develop fast detectors and properly understand time response features. The present open-source software, for example, Weightfield2 [19] and KDetSim [20] are only available for silicon detectors. The corresponding simulation tool for silicon carbide detectors is lacking due to distinct material parameters. Therefore, we also developed a fast simulation software termed RASER [21] for applications with silicon carbide detectors, which was used in this study to reproduce measured data.

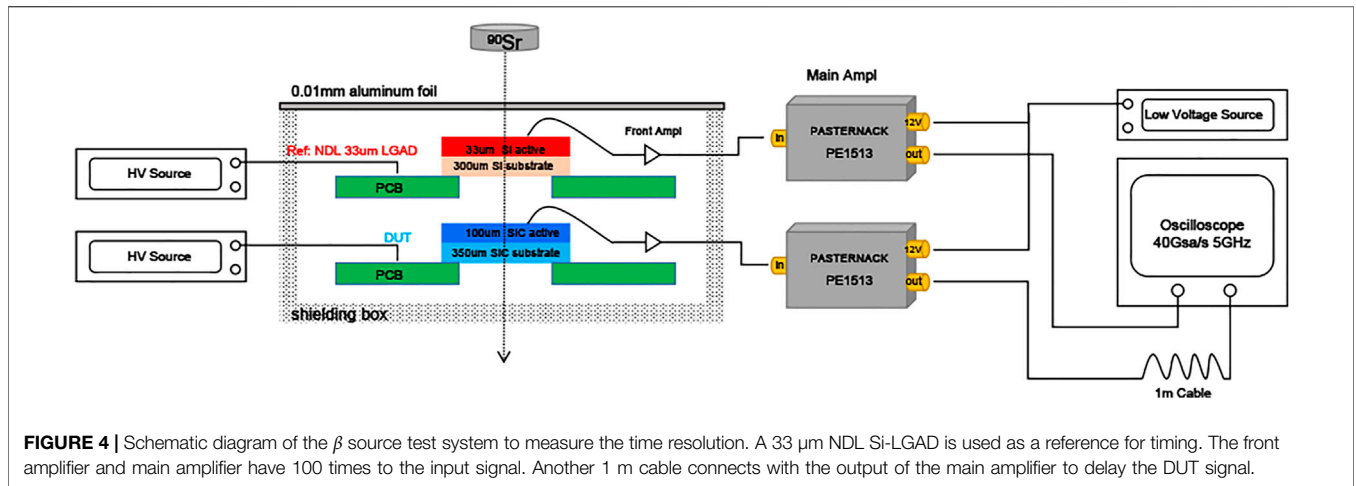


**FIGURE 4** | Schematic diagram of the  $\beta$  source test system to measure the time resolution. A 33  $\mu\text{m}$  NDL Si-LGAD is used as a reference for timing. The front amplifier and main amplifier have 100 times to the input signal. Another 1 m cable connects with the output of the main amplifier to delay the DUT signal.

## THE DEVICE UNDER INVESTIGATION

The 4H-SiC PIN devices under investigation are fabricated by Nanjing University and come in two different sizes: 5 mm  $\times$  5 mm and 1.5 mm  $\times$  1.5 mm. **Figure 1** shows the 5 mm  $\times$  5 mm sample which has two ohmic contacts on the top and bottom. The two devices both have a 100  $\mu\text{m}$  high resistive active 4H-SiC epitaxy layer and 350  $\mu\text{m}$  substrate, whereas the effective doping concentration is different: we have  $N_{\text{eff}}$  (5 mm  $\times$  5 mm) =  $5.2 \times 10^{13} \text{ cm}^{-3}$  and  $N_{\text{eff}}$  (1.5 mm  $\times$  1.5 mm) =  $2.7 \times 10^{13} \text{ cm}^{-3}$ , respectively. These values may be extracted from the capacitance–voltage curve (see **Figure 2**) by

$$N_{\text{eff}} = \frac{2}{q\epsilon A^2 d(1/C^2)/dV} \quad (1)$$

where  $q$  is the electron charge,  $\epsilon$  is the dielectric constant of 4H-SiC, and  $A$  is the area of the active region. Taking into account the doping levels and the dependence on device thickness  $V_{\text{dep}} = \frac{q|N_{\text{eff}}|d^2}{2\epsilon}$  with  $d = 100 \mu\text{m}$ , the full depleted voltages are given by  $V_{\text{dep}}$  (5 mm  $\times$  5 mm) = 484 V and  $V_{\text{dep}}$  (1.5 mm  $\times$  1.5 mm) = 248 V.

The current–voltage characteristics are shown in **Figure 3**. The typical unidirectional conduction characteristic of PINs is observed, and the breakdown voltage is larger than 800 V for both sizes. A higher leakage current may be collected by the 5 mm $\times$ 5 mm size device due to its larger volume. The leakage current density is  $J < 100 \text{ nA/cm}^2$  for both the devices with a 500 V reverse voltage, where  $J$  (5 mm  $\times$  5 mm) =  $63.2 \text{ nA/cm}^2$  and  $J$  (1.5 mm  $\times$  1.5 mm) =  $34.6 \text{ nA/cm}^2$ . The lower current density of the smaller device agrees with its lower effective doping concentration, as obtained from data in **Figure 2**.

## EXPERIMENTAL SETUP

### $\beta$ Source Test System

A schematic diagram of the experimental setup to determine the time resolution of 4H-SiC detectors is shown in **Figure 4**. We choose a 33  $\mu\text{m}$  silicon LGAD as the reference timing

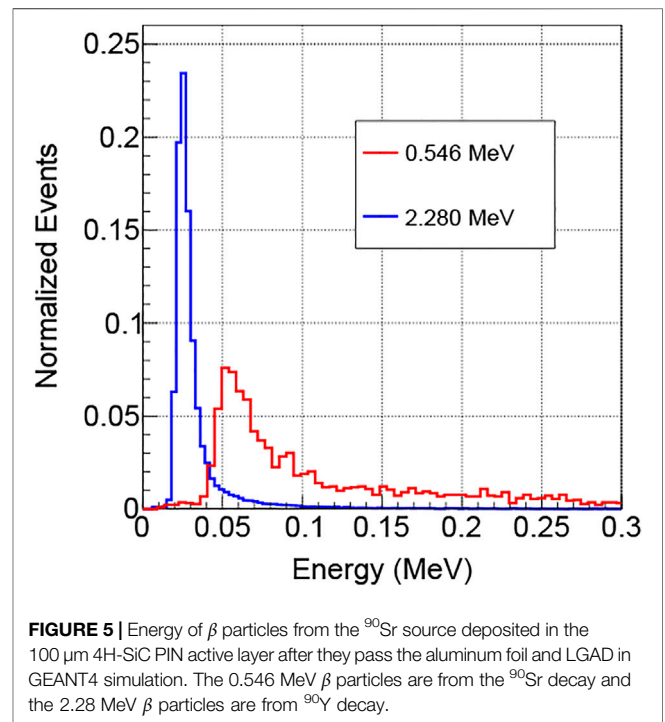


**FIGURE 5** | Energy of  $\beta$  particles from the  $^{90}\text{Sr}$  source deposited in the 100  $\mu\text{m}$  4H-SiC PIN active layer after they pass the aluminum foil and LGAD in GEANT4 simulation. The 0.546 MeV  $\beta$  particles are from the  $^{90}\text{Sr}$  decay and the 2.28 MeV  $\beta$  particles are from  $^{90}\text{Y}$  decay.

device owing to its 34 ps time resolution at  $U = 200 \text{ V}$  and room temperature. The reference timing device is developed by the Institute of High Energy Physics (IHEP) of Chinese Academic Sciences and the Novel Device Laboratory (NDL) of Beijing Normal University [22–24]. The  $^{90}\text{Sr}$  source emits  $\beta$  particles at 0.546 MeV from  $^{90}\text{Sr}$  and at 2.280 MeV from  $^{90}\text{Y}$ . Both are able to penetrate the LGAD device and deposit energy in the 4H-SiC detector. The front side readout boards are designed for LGAD devices by the University of California, Santa Cruz (UCSC). Each board has a 2 mm diameter hole in the middle. The overall front side electronics are transferred into a metal box to shield it from electromagnetic interference, with a 0.01 mm aluminum foil covering. Two 20 dB broadband amplifiers are placed before the oscilloscope to enhance the SNR. There is an additional 1 m

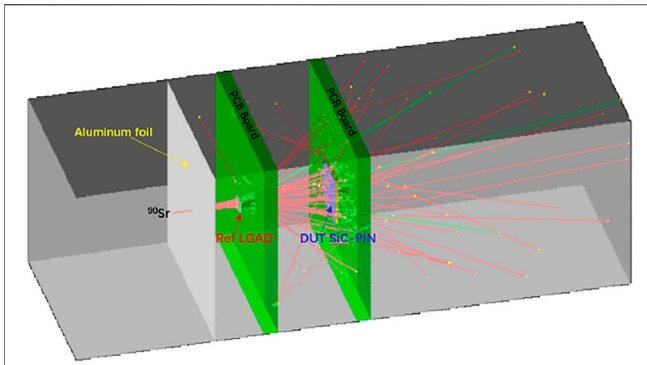


**FIGURE 6** | Scattering of  $\beta$  particles with 2.28 MeV after the aluminum foil and LGAD in GEANT4 simulations. The figure shows the tracks of 50 incident particles going through the entire  $\beta$  source test system.

cable on the DUT side to delay the signal (by  $\sim 5$  ns) and enhance trigger efficiency. The sampling rate of the oscilloscope is 40 GSa/s, and each channel has 20 GSa/s.

### Energy Response by GEANT4 Simulation

To analyze the energy loss of MIPs in  $100 \mu\text{m}$  4H-SiC active layer tallies, we use a simulation based on GEANT4, which allows one to describe the energy deposition. **Figure 5** describes the energy deposition of the  $\beta$  particle in the  $100 \mu\text{m}$  4H-SiC active layer in the system (see **Figure 6**). The energy loss in the aluminum foil may be neglected. The scattering of  $\beta$  particles in the aluminum foil and LGAD strongly decreases trigger efficiency for the 4H-SiC device. In turn, this explains the difference of trigger efficiency between the  $5 \text{ mm} \times 5 \text{ mm}$  (4.7 events/min) and the  $1.5 \text{ mm} \times 1.5 \text{ mm}$  (2.1 events/min) samples since a larger size corresponds to higher trigger efficiency. The most probable values (MPVs) of the energy deposition in  $100 \mu\text{m}$  4H-SiC layer are 25 and 55 MeV for the two different energy  $\beta$  particles from the  $^{90}\text{Sr}$  source. There are little differences with the previous experimental result ( $\sim 42$  MeV) [25] due to scattering

effects by the aluminum foil and LGAD, which make the ionization track slightly longer than  $100 \mu\text{m}$ , but the average MPV of energy deposition from these two particles is close to the experimental result.

## TIME RESOLUTION OF 4H-SiC PIN

### Waveform Sampling

The two channels are triggered at the same time with different trigger levels for waveform sampling.  $\text{Trigger}_{Ref} = 25 \text{ mV}$  and  $\text{trigger}_{DUT} = 15 \text{ mV}$  are determined by noise levels (see **Figure 7**) to suppress noise spikes. **Figure 8** shows the waveforms from the LGAD (Ref) and 4H-SiC PIN (DUT), respectively. The time delay,  $\sim 5$  ns, is obtained using an additional 1 m cable and is there to enhance trigger efficiency. Owing to internal gain in the LGAD, the signal of the LGAD is higher than that of 4H-SiC PIN despite the LGAD having a thinner active layer. The time resolution of the NDL LGAD is  $\sigma_{Ref} = 34 \pm 1 \text{ ps}$  when the bias voltage is  $U = 200 \text{ V}$  [24].

### Time Resolution

The time resolution obtained with different device sizes and reverse voltages are studied here considering the influence of capacitance and carrier velocity. For the timing method, the constant fraction discrimination (CFD) is adopted with a fraction equal to 0.5. **Figure 9** show the distribution of  $\Delta T = T_{DUT} - T_{Ref}$  for different device sizes and reverse voltages. The time resolution of DUT could be extracted by  $\sigma_{DUT} = \sqrt{\sigma_{\Delta T}^2 - \sigma_{Ref}^2}$ , where  $\sigma(5 \text{ mm} \times 5 \text{ mm}, U = 500 \text{ V}) = 94 \pm 1 \text{ ps}$ ,  $\sigma(5 \text{ mm} \times 5 \text{ mm}, U = 300 \text{ V}) = 103 \pm 1 \text{ ps}$ , and  $\sigma(1.5 \times 1.5 \text{ mm}, U = 300 \text{ V}) = 96 \pm 2 \text{ ps}$ .

At fixed size, 4H-SiC-PIN ( $5 \times 5 \text{ mm}$ ) shows better time resolution using higher reverse voltage due to faster carrier velocity. At fixed reverse voltage, faster rising time caused by smaller capacitance improves the time resolution if the influence of the undepleted thickness in the  $5 \times 5 \text{ mm}$  size device may be neglected. Meanwhile, the mean of  $\Delta T$  shifts from 5.03 to 4.81 ns for different size devices due to faster rising time of devices with

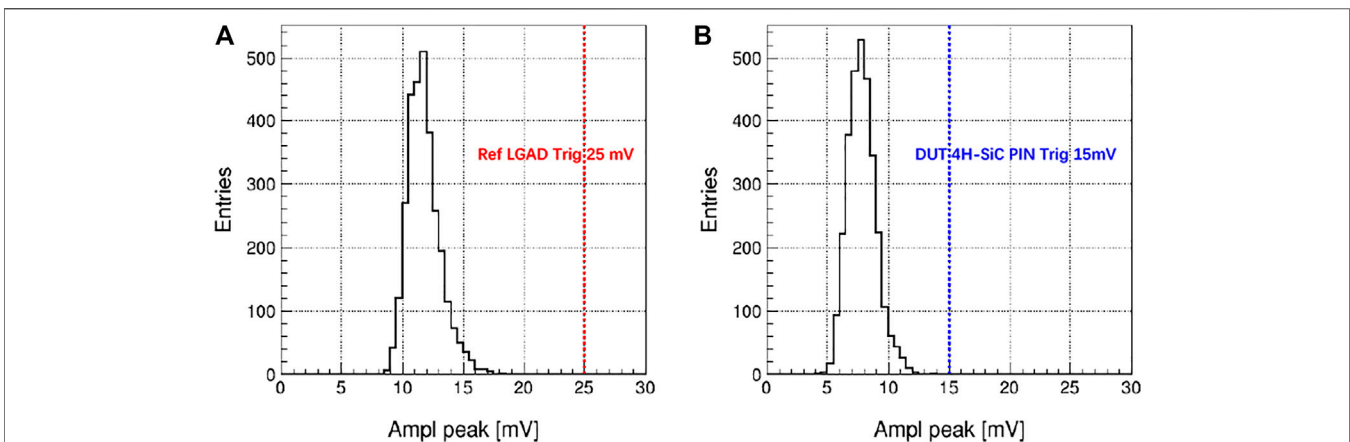


**FIGURE 7** | Peak amplitude distribution of noise for **(A)**  $33 \mu\text{m}$  Si LGAD with bias voltage  $U = 200 \text{ V}$  and **(B)**  $100 \mu\text{m}$  4H-SiC PIN with  $U = 500 \text{ V}$ . The trigger levels are chosen to eliminate the fake signals from noise spikes.

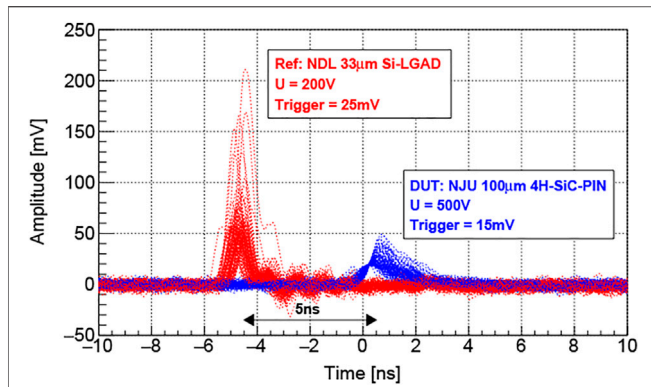


**FIGURE 8 |** Waveform sampling for Si-LGAD (red) and 4H-SiC-PIN (blue) as collected by an oscilloscope. The trigger thresholds are determined by the noise level to eliminate all noise spikes. The ~5 ns time delay of 4H-SiC-PIN signals is caused by the additional, 1 m long cable.

smaller capacitance. As it is apparent in **Figure 10**, a ~400 ps difference in the rising time leads to a ~200 ps time-shifting with 0.5 CFD fraction.

## SIMULATION

### Introduction of Fast Simulation Tool—RASER

We have developed a fast simulation tool, termed RASER, to study the time resolution performance of SiC detectors [21]. We use FEniCS [26], an open-source computing platform for solving partial differential equations (PDEs) to calculate the electric field and weighting potential of SiC detectors. MIPs with nonuniform charge deposition and amplitude variability are considered. The induced current is calculated by Shockley–Ramo’s theorem [27] where the carrier drift is simulated using 0.1 μm steps and taking into account both magnetic field and thermal diffusion. We also assume the use of a simplified charge-sensitive amplifier (CSA) for the read-out [28].

### Weighting Field Potentials and Electric Field Calculation by FEniCS

The electric potential and weighting potential can be computed by solving Poisson’s and Laplace’s equations:

$$\nabla^2 \vec{U}(r) = \frac{\rho}{\epsilon}, \quad (2)$$

$$\nabla^2 \vec{U}_w(r) = 0, \quad (3)$$

where  $\vec{U}(r)$  is the electric potential,  $\vec{U}_w(r)$  is the weighting potential,  $\epsilon$  is the electric permittivity of SiC, and  $\rho$  is the charge density. The electric and weighting field are then denoted as  $\vec{E}(r) = -\nabla \vec{U}(r)$  and  $\vec{E}_w(r) = -\nabla \vec{U}_w(r)$ , respectively.

### Current Calculation

The induced current in the SiC detector is produced by the motion of the electron-hole pairs. The current appears when

electron-hole pairs begin to move and disappears when all the pairs reach the electrode or the boundary of the detector. The instantaneous current induced by an electron or a hole can be calculated with Shockley–Ramo’s theorem:

$$I = -q\vec{v}(r) \cdot \vec{E}_w(r), \quad (4)$$

where  $r$  is the position of the electron or hole,  $\vec{v}(r)$  is the drift velocity, and  $\vec{E}_w(r)$  is the weighting potential. The drift velocity  $\vec{v}(r)$  is given by  $\mu_{SiC} \cdot \vec{E}(r)$ , where  $\mu_{SiC}$  is the mobility in SiC. The mobility model of SiC in RASER is based on [29], and the sum of the currents induced by all electrons and holes is the total current. In the simulation, the influence of nonuniform charge deposition and impact position on the time resolution is simulated by GEANT4. The simulation contained the divergence angle from the scattering of (**Figure 4**) the upper PCB board, aluminum foil, and LGAD detector.

### Comparison Between the Simulated and Measured Time Resolution

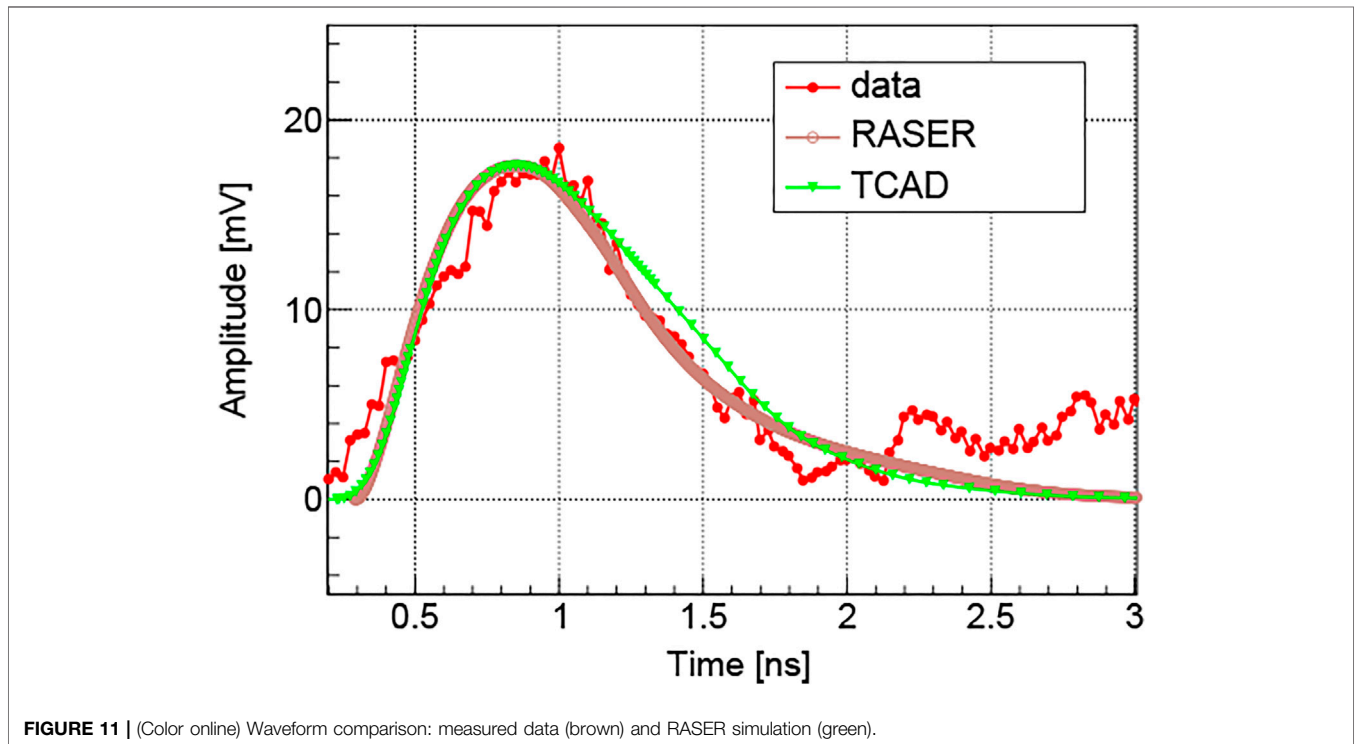
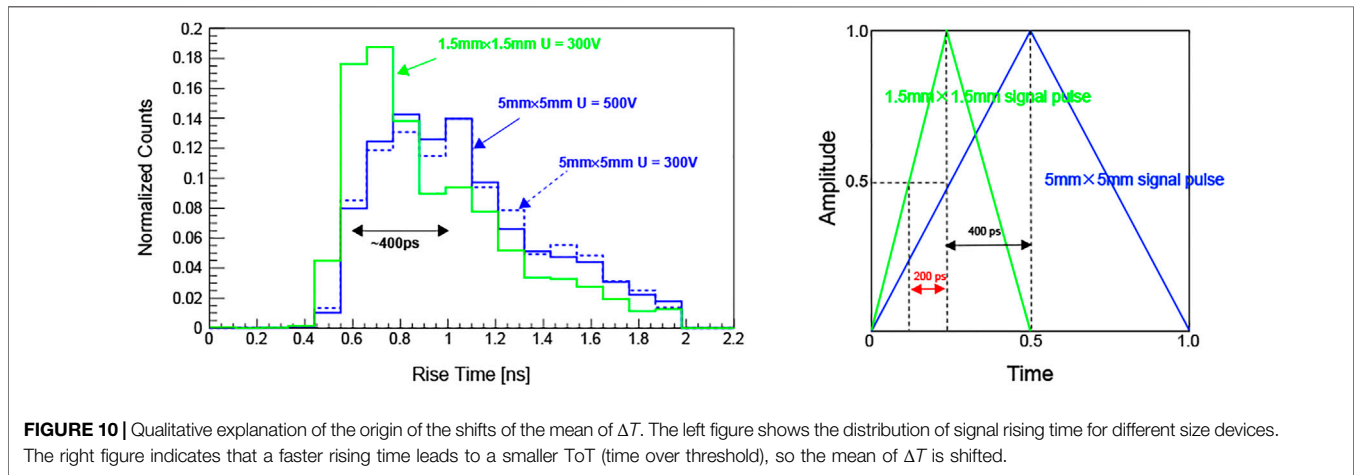
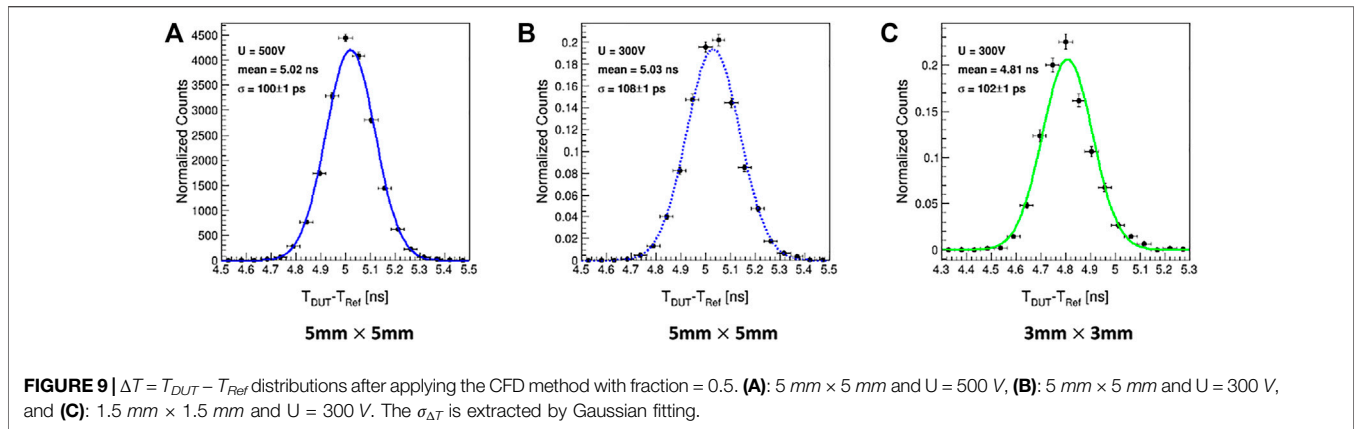
The time resolution of the SiC detector can be expressed as follows [13]:

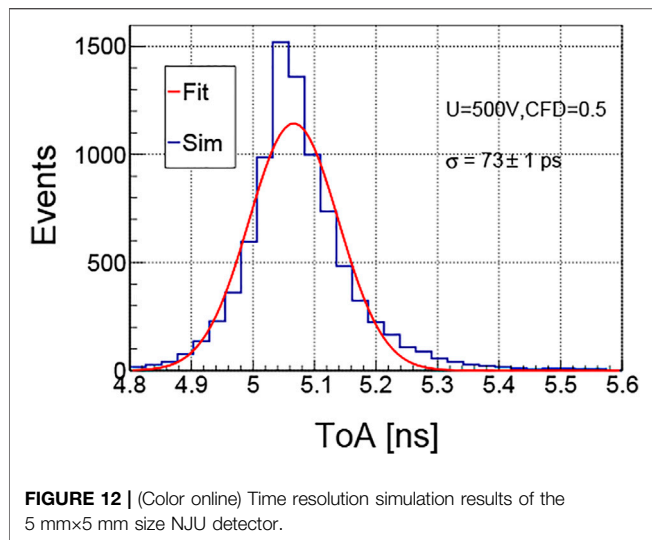
$$\sigma_t^2 = \sigma_{Time\ Walk}^2 + \sigma_{Landau\ Noise}^2 + \sigma_{Distortion}^2 + \sigma_{Jitter}^2 + \sigma_{TDC}^2, \quad (5)$$

where the correlations among the different items are ignored. In simulations, the time walk  $\sigma_{Time\ Walk}$  is dominated by Landau variation in signal amplitude and is eliminated by the CFD method. The nonuniform charge deposition and scattering effects cause Landau noise  $\sigma_{Landau\ Noise}$ . The nonuniform weighting potential and the electric field cause signal distortion  $\sigma_{Distortion}$ . The electronics noise, which leads to  $\sigma_{Jitter}$  and  $\sigma_{TDC}$ , is dominated by the binning of signal waveforms. All these time resolution contributions, except the distortion term, are considered in the simulation process.

We simulated the time resolution of the NJU detector with 5 mm × 5 mm sizes with a 500 V bias voltage at room temperature  $T = 300\ K$ . In these conditions, the average carrier velocities are  $V_{electron} = 150\ \mu m/ns$  and  $V_{hole} = 50\ \mu m/ns$ . We use RASER to model an ideal planar detector and calculate the electric field so that  $\sigma_{Distortion}$  is not considered in the simulation. Based on GEANT4 simulation, the nonuniform charge deposition and scattering effects are applied in RASER to reproduce the contribution of  $\sigma_{Landau\ Noise}$ . The random noise is added in each signal waveform to estimate  $\sigma_{Jitter}$ . The contribution of  $\sigma_{TDC}$  has been considered in binning the signal (the same bin interval 50 ps/bin with sampling time step). The program has been validated by comparing the induced current for MIPs of RASER simulations and measured signals. **Figure 11** shows the comparison between waveforms obtained from RASER and TCAD simulation and measured data, where the mobility model applied in TCAD is the Masetti model with parameters from [30, 31]. Good consistency is found in all three cases.

The results of simulations for the time resolution of the NJU detector are shown in **Figure 12**. We use 20,000 events, and the same CFD fraction 0.5 as in the measurements is used to obtain





the time of arrival (ToA). The time resolution obtained by Gaussian fitting is  $(73 \pm 1 \text{ ps})$ , where the simulated  $\sigma_{\text{Jitter}}$  is  $66 \text{ ps}$  and leftover  $\sigma_{\text{Landau Noise}}$  and  $\sigma_{\text{TDC}}$  is  $30 \text{ ps}$  in total due to  $\sigma_{\text{Time Walk}}$  being absent. The simulated time resolution is  $(24 \pm 1) \text{ ps}$  less than the measurement result. The origins of this difference are likely because there is no shielding box of the beta source measurement, which leads to an increase in time resolution. RASER software can effectively simulate the time resolution of SiC to some extent, but measurements and simulations both need further optimization.

## CONCLUSION

The best time resolution of the NJU 5 mm×5 mm 4H-SiC-PIN detector with the  $^{90}\text{Sr}$  source is  $94 \pm 1 \text{ ps}$ . On using higher reverse voltage and smaller capacitance, better time resolution is obtained. The waveform simulated by RASER has been validated against measurements. The simulated time resolution indicates that all the leading contributions of the test system should be considered to obtain reliable results. Our study about measured and simulated time resolutions is useful to develop ultrafast 4H-SiC LGAD and 3D 4H-SiC detectors

## REFERENCES

1. RD50 Collaboration. *RD50 Prolongation Request* (2018).
2. Moll M Displacement Damage in Silicon Detectors for High Energy Physics. *IEEE Trans Nucl Sci* (2018) PP:1. doi:10.1109/tns.2018.2819506
3. Adam W, Berdermann E, Bergonzo P, Boer WD, Bogani F, Borchini E, et al. The Development of diamond Tracking Detectors for the LHC. *Nucl Instrum Methods A* (2003) 514:79–86.
4. Reichmann MP, Alexopoulos A, Artuso M, Bachmair F, Zavrtanik M Diamond Detector Technology: Status and Perspectives. *Eur Phys Soc Conf High Energy Phys* (2017).
5. Rafi JM, Pellegrini G, Godignon P, Ugobono SO, Rius G, Tsunoda I, et al. Electron, Neutron, and Proton Irradiation Effects on SiC Radiation

[32] which are expected to achieve improved time resolution in the near future.

## DATA AVAILABILITY STATEMENT

The raw data supporting the conclusion of this article will be made available by the authors, without undue reservation.

## AUTHOR CONTRIBUTIONS

Conceptualization: XS. Experimental setup and measurement: TY, JZ, and SX. Software development: TY, YT, SX, KL, RK, and JL. TCAD Simulation: TY and BW. Developing the SiC sample: HL and QL. Writing and original draft preparation: TY and YT. Supervision: MZ, XZ, and CW. All authors have read and agreed to the published version of the manuscript.

## FUNDING

This research is supported by the National Natural Science Foundation of China (No.11961141014); and the Program of Science and Technology Development Plan of Jilin Province of China under Contract No. 20210508047RQ.

## ACKNOWLEDGMENTS

This work is carried out in the CERN RD50 framework. We would like to acknowledge the TeledyneLecroy Beijing office for providing us with a fast sampling oscilloscope, Gregor Kramberger for helpful discussions about the simulation method in KDetSim, and the IHEP HGTD group for the hardware support and for the suggestions concerning time resolution measurements.

## SUPPLEMENTARY MATERIAL

The Supplementary Material for this article can be found online at: <https://www.frontiersin.org/articles/10.3389/fphy.2022.718071/full#supplementary-material>

Detectors. *IEEE Trans Nucl Sci* (2020) 67:2481–9. doi:10.1109/TNS.2020.3029730

6. Liu L, Liu A, Bai S, Lv L, Jin P, Ouyang X Radiation Resistance of Silicon Carbide Schottky Diode Detectors in D-T Fusion Neutron Detection. *Sci Rep* (2017) 7:13376. doi:10.1038/s41598-017-13715-3
7. Cai X, Zhou D, Yang S, Lu H, Chen D, Ren F, et al. 4H-SiC SACM Avalanche Photodiode with Low Breakdown Voltage and High UV Detection Efficiency. *IEEE Photon J.* (2016) 8:1–7. doi:10.1109/jphot.2016.2614499
8. Zweben S, Budny RV, Darrow DS, Medley SS, Nazikian R, Stratton BC, et al. Special Topic Alpha Particle Physics Experiments in the Tokamak Fusion Test Reactor. *Nucl Fusion* (2000) 40:1. doi:10.2172/2545
9. Moscatelli F, Scorzoni A, Poggi A, Bruzzi M, Sciortino S, Lagomarsino S, et al. Radiation Hardness after Very High Neutron Irradiation of Minimum Ionizing Particle Detectors Based on 4H-SiC P/sup +/n

- Junctions. *IEEE Trans Nucl Sci* (2006) 53:1557–63. doi:10.1109/tns.2006.872202
10. Zhang X, Cates JW, Hayward JP, Bertuccio G, Puglisi D, Hausladen PA Characterizing the Timing Performance of a Fast 4H-SiC Detector with an  $^{241}\text{Am}$  Source. *IEEE Trans Nucl Sci* (2013) 60:2352–6. doi:10.1109/tns.2013.2260652
  11. Akchurin N, Ciriolo V, Currás E, Damgov J, Fernández M, Gallrapp C, et al. On the Timing Performance of Thin Planar Silicon Sensors. *Nucl Instr Methods Phys Res Section A: Acc Spectrometers, Detectors Associated Equipment* (2017) 859:31–6. doi:10.1016/j.nima.2017.03.065
  12. Benoit M, Cardarelli R, Débieux S, Favre Y, Iacobucci G, Nessi M, et al. 100ps Time Resolution with Thin Silicon Pixel Detectors and a Sige Hbt Amplifier. *J Instrumentation* (2015) 11:P03011. doi:10.1088/1748-0221/11/03/P03011
  13. Sadrozinski HF, Seiden A, Cartiglia N. 4D Tracking with Ultra-fast Silicon Detectors. *Rep Prog Phys* (2018) 81:026101. doi:10.1088/1361-6633/aa94d3
  14. Sola V, Arcidiaconob R, Boscardinde M, Cartigliab N, Dalla Bettafe G-F, Ficorellade F, et al. First FBK production of 50 um ultra-fast silicon detectors. *Nucl Instrum Methods A* (2019) 924:360. doi:10.1016/j.nima.2018.07.060
  15. Giacomini G, Chen W, Lanni F, Tricoli A. Development of a Technology for the Fabrication of Low-Gain Avalanche Diodes at BNL. *Nucl Instrum Methods A* (2019) 934:73. doi:10.1016/j.nima.2019.04.073
  16. Pellegrini G, Fernández-Martínez P, Baselgaa M, Fletaa C, Floresa D, Grecoa V, et al. Technology Developments and First Measurements of Low Gain Avalanche Detectors (LGAD) for High Energy Physics Applications. *Nucl Instrum Methods A* (2014) 765:12. doi:10.1016/j.nima.2014.06.008
  17. Fan Y, Alderweireldt S, Agapopoulou C, Atanov N, Ayoub MK, Caforio D, et al. Radiation Hardness of the Low Gain Avalanche Diodes Developed by NDL and IHEP in China. *Nucl Instrum Methods A* (2020) 984:164608. doi:10.1016/j.nima.2020.164608
  18. Tan Y, Yang T, Xiao S, Wu K, Wang L, Lie Y, et al. Radiation Effects on NDL Prototype LGAD Sensors after Proton Irradiation. *Nucl Instrum Methods A* (2021) 1010:165559. doi:10.1016/j.nima.2021.165559
  19. Cenna F, Cartiglia N, Friedl M, Kolbinger B, Sadrozinski HFW, Seiden A, et al. Weightfield2: A Fast Simulator for Silicon and diamond Solid State Detector. *Nucl Instr Methods Phys Res Section A: Acc Spectrometers, Detectors Associated Equipment* (2015) 796:149–53. doi:10.1016/j.nima.2015.04.015
  20. Kramberger G, Cindro V, Flores D, Hidalgo S, Hiti B, Manna M, et al. Timing Performance of Small Cell 3D Silicon Detectors. *Nucl Instr Methods Phys Res Section A: Acc Spectrometers, Detectors Associated Equipment* (2019) 934:26–32. doi:10.1016/j.nima.2019.04.088
  21. Shi X, Tan Y, Yang T, Liu K, Kiuchi R, Lin J, et al. RASER v2.2.1 (2021). Available from: <https://pypi.org/project/raser/>. [Accessed October 08, 2021].
  22. Yang Y, Suyu X, Yunyun F, Dejun H, Zhijun L, Baohua Q, et al. Characterization of the First Prototype Ndl Low Gain Avalanche Detectors (LGAD). *Nucl Instrum Methods A* (2021) 1011:165591. doi:10.1016/j.nima.2021.165591
  23. Xiao S, Alderweireldt S, Ali S, Allaire C, Agapopoulou C, Atanov N, et al. Beam Test Results of NDL Low Gain Avalanche Detectors (LGAD). *Nucl Instrum Methods A* (2021) 989:164956. doi:10.1016/j.nima.2020.164956
  24. Li M, Cui H, Fan Y, Han D, Heng Y, Li S, et al. The Timing Resolution of IHEP-NDL LGAD Sensors with Different Active Layer Thicknesses. *IEEE Trans Nucl Sci* (2021) 68:2309–14. doi:10.1109/tns.2021.3097746
  25. Kalinina EV, Kossov VG, Strokan NB, Ivanov AM, Yafaev RR, Kholuyanov GF Spectrometric Properties of SiC Detectors Based on Ion-Implanted P +n Junctions. *Semiconductors* (2006) 40:1096–100. doi:10.1134/s1063782606090193
  26. Langtangen HP, Logg A *Solving PDEs in Python – the FEniCS Tutorial Volume I* (2017).
  27. Ramo S Currents Induced by Electron Motion. *Proc IRE* (1939) 27:584–5. doi:10.1109/jrproc.1939.228757
  28. Sadrozinski HFW, Anker A, Chen J, Fadeyev V, Freeman P, Galloway Z, et al. Ultra-fast Silicon Detectors (UFS). *Nucl Instr Methods Phys Res Section A: Acc Spectrometers, Detectors Associated Equipment* (2016) 831:18–23. doi:10.1016/j.nima.2016.03.093
  29. Das A, Dutttagupta SP TCAD Simulation for Alpha-Particle Spectroscopy Using SiC Schottky Diode. *Radiat Prot Dosimetry* (2015) 167:443–52. doi:10.1093/rpd/ncu369
  30. Schaffer WJ, Negley GH, Irvine KG, Palmour JW Conductivity Anisotropy in Epitaxial 6H and 4H SiC. *MRS Online Proceeding Libr Archive* (1994) 339:595. doi:10.1557/proc-339-595
  31. Ayalew T. *SiC Semiconductor Devices, Technology, Modeling, and Simulation*. Ph.D. thesis. Austria: Technischen Universitaet Wien (2004).
  32. Tan Y, Yang T, Liu K, Wang C, Zhang X, Zhao M, et al. Timing Performance Simulation for 3D 4H-SiC Detector. *Micromachines* (2022) 13. doi:10.3390/mi13010046

**Conflict of Interest:** The authors declare that the research was conducted in the absence of any commercial or financial relationships that could be construed as a potential conflict of interest.

**Publisher's Note:** All claims expressed in this article are solely those of the authors and do not necessarily represent those of their affiliated organizations, or those of the publisher, the editors, and the reviewers. Any product that may be evaluated in this article, or claim that may be made by its manufacturer, is not guaranteed or endorsed by the publisher.

Copyright © 2022 Yang, Tan, Liu, Xiao, Liu, Zhang, Kiuchi, Zhao, Zhang, Wang, Wu, Lin, Song, Lu and Shi. This is an open-access article distributed under the terms of the Creative Commons Attribution License (CC BY). The use, distribution or reproduction in other forums is permitted, provided the original author(s) and the copyright owner(s) are credited and that the original publication in this journal is cited, in accordance with accepted academic practice. No use, distribution or reproduction is permitted which does not comply with these terms.